

**SURFACE ROUGHNESS EFFECTS ON CIRCULAR CYLINDERS AT HIGH REYNOLDS NUMBERS.**

**M. Eaddy, W.H. Melbourne, J. Sheridan**  
Department of Mechanical Engineering  
Monash University  
Australia

**ABSTRACT**

The problem of flow-induced vibration has been studied extensively. However, much of this research has focused on the smooth cylinder to gain an understanding of the mechanisms that cause vortex-induced vibration. In this paper results of an investigation of the effect of surface roughness on the cross-wind forces are presented. Measurements of the sectional RMS fluctuating lift forces and the axial correlation of the pressures for Reynolds numbers from  $1 \times 10^5$  to  $1.4 \times 10^6$  are given. It was found that surface roughness significantly increased the axial correlation of the pressures to similar values found at high subcritical Reynolds numbers. There was little effect of the surface roughness on the sectional lift forces. The improved correlation of the vortex shedding means rough cylinders will be subject to larger cross-wind forces and an increased possibility of vortex-induced vibration compared to smooth cylinders.

**INTRODUCTION**

The problem of vortex-induced vibration confronts us in many everyday situations; from the vibration of a domestic television aerial to flow over heat exchanger tube banks to large towers, and in some situations left untreated can lead to structure failures. The importance of finding causes and solutions to vortex induced vibration is reflected in the quantity of research.

Many of the circular cylinder applications mentioned in the previous paragraph are not highly polished, instead they have a degree of surface roughness caused by manufacturing tolerances or environmental conditions. Research on smooth cylinders in low turbulence flow has shown the fluid-structure mechanisms that result in vibration over a wide range of Reynolds numbers. However, the quantity of research data available showing the effect of surface roughness and

turbulence is limited, particularly above Reynolds numbers of  $10^5$ .

Research has shown, at a Reynolds number of approximately  $10^5$ , the flow field around a smooth cylinder undergoes rapid change, known as 'critical transition' [1]. This transition has been shown to be very sensitive to perturbations in the flow or on the cylinder surface and their presence will cause the transition to occur at a lower Reynolds number [2, 3]. The trend highlighted the possibility of using roughened cylinders as a method of simulating postcritical and higher Reynolds numbers in subcritical experimental facilities. Numerous measurements of the mean drag coefficient and vortex shedding spectra have been published, but little data is available on the effect of roughness on the crosswind lift and axial correlation of the forces [4-7].

Cheung [8] carried out a detailed investigation into the effects of surface roughness and free stream turbulence, identifying the significant influence of surface roughness on the total lift forces. Zhang [9] followed Cheung's investigation examining the possibility of regime simulation using surface roughness at higher Reynolds numbers. He found, like the authors mentioned above, that the surface roughness did promote an earlier return to regular vortex shedding. Accompanying this return to regular vortex shedding, Zhang found there was an increase in the total RMS fluctuating lift compared to a smooth cylinder, which also increased with relative roughness. However, the total forces are an integrated effect of the sectional forces and their correlation along the cylinder, making it impossible to determine whether the sectional lift force or the correlation was increasing. Zhang [9] and Shih *et al.* [10] observed that there was a significant increase in the crosswind vibration during the rough cylinder experiments that suggests that the vortex shedding became more coherent on the rough cylinders.

Measurement of the axial correlation of the lift forces by Batham [11] and Ribeiro [7] has shed some light on the mechanism causing the increased vibration. The two authors measured axial correlation lengths of three diameters on roughened cylinders, which are similar to those measured on smooth cylinders at high sub-critical Reynolds numbers. However, these are the only sets of data on rough cylinders above Reynolds numbers of  $10^5$  and are limited to  $2.5 \times 10^5$ . ESDU [12] plots this data and extrapolates to much higher Reynolds numbers. However, there are no experimental data at these higher Reynolds numbers to confirm the extrapolated trend.

In this paper we present part of the results of an investigation into the effects of surface roughness on the sectional cross-wind forces of a circular cylinder. Mean drag coefficients, sectional RMS fluctuating lift coefficients and pressure correlation coefficients for Reynolds numbers from  $1 \times 10^5$  to  $1.4 \times 10^6$  are presented.

## NOMENCLATURE

- $C_D$  – Mean drag coefficient
- $C_p$  – Pressure coefficient
- $D$  – Cylinder diameter
- $I$  – Turbulence intensity
- $ID$  – Internal Diameter
- $k$  – Roughness factor
- $l$  – Cylinder Length
- $L_x$  – Longitudinal integral length scale of turbulence
- $P_x$  – Fluctuating pressure of signal  $x$
- $RMS$  – Root Mean Square
- $\rho_{xy}$  – Correlation coefficient
- $\sigma_x$  – Standard deviation of signal  $x$

## MODELS AND METHODS

### Wind Tunnel

The experiments were performed in two wind tunnels at Monash University. The 100 mm cylinders were tested in the 2x1 m section of the 450 kW wind tunnel and the 400 mm and 630 mm cylinders were tested in the 4x5 m section of the 1.5 MW wind tunnel.

The tunnels had a mean velocity profile within 3 % across the axis of the cylinders mounting position. The bare tunnel turbulence intensity of the 450 kW and 1.5 MW wind tunnels were 0.6 % and 3 % respectively. In order to compare results between the tunnels a turbulence grid was installed in the 450 kW wind tunnel to increase  $I = 3$  %. The  $L_x$  values for the tunnels were 70 mm and 210 mm for the 450 kW and 1.5 MW respectively.

### Cylinder Models

Four 100 mm aluminum cylinders were instrumented with a total of 86 pressure taps. The taps were arranged as follows; a complete central ring with taps at 10-degree intervals, taps at ratios of 0.25, 0.5, 1, 2 and 3 diameters either side of the central

ring were placed along the 90 and 270 degree generators (0 degrees is the front stagnation point) and a partial ring of taps  $2D$  to the side of the central ring. The 400 and 630 mm cylinders were instrumented with 157 taps with a similar tap configuration as the 100 mm cylinders. Extra complete rings of taps were installed at  $1D$  and  $2D$  to the side of the central ring. The taps were always inserted in the wall of the cylinder level with either the surface of the cylinder in the case of the smooth configuration, or level with the outside of the backing paper of the sandpaper in the case of the rough configurations. No clearance holes or gaps were left around the taps on the rough cylinder with the roughness elements continuing up to the edge of the pressure taps. The current paper reports the results from the central ring and generators. Future papers will report all the experimental results fully.

The taps were connected to electronic Scanivalve transducers via closed PVC tubing. The tubes were 1500 mm long x 1.5 mm  $ID$  and 5000 mm x 3 mm  $ID$  for the 100 mm and 400 and 630 mm cylinders respectively. No restrictors or leak tube systems were used to reduce the pressure tubing resonant effects on the fluctuating pressures; corrections were made using digitally using transfer functions.

Surface roughness was simulated using different grades of commercial sandpaper. Table 1 summarizes the relative roughness for the different cylinders. The roughness factor  $k$  was taken as the average particle size of the grit on the sandpaper and normalized by the cylinder diameter to determine the relative roughness. SIA Abrasives manufacturer their sandpaper to the FEPA-standard 43-1984 R 1993, which estimates the average particle size required for a particular grade of sandpaper.

**Table 1: Cylinder relative roughness**

Cylinder Diameter (mm)	Sandpaper Grade	$k / D$
100	P180	$0.82 \times 10^{-3}$
100	P60	$2.69 \times 10^{-3}$
100	P40	$4.25 \times 10^{-3}$
630	P36	$0.85 \times 10^{-3}$
630	P16	$2.10 \times 10^{-3}$

For the smooth cylinder configurations, the cylinder surfaces were sanded to remove any major manufacturing imperfections, but were not polished.

The cylinders were installed horizontally at mid section height and fixed to the walls of the wind tunnels. End plates were used to maintain a two-dimensional flow. The characteristics of the cylinders when installed in the wind tunnels are summarized in Table 2.

**Table 2: Cylinder characteristics**

Cylinder (mm)	Aspect Ratio (1 / D)	Blockage (%)	Natural Frequency (Hz)
100	9.1	5	210
400	9.0	8	18
630	6.0	12	16

**Instrumentation and Data Analysis**

The fluctuating pressures were sampled using an electronic Scanivalve pressure system. The sampling rate and sample time were 1000 Hz for 35 seconds for the 100 mm cylinders and 200 Hz for 120 seconds on the 400 and 630 mm cylinders. The pressures were recorded on hard disk for post processing.

The pressure data consisted was first corrected for the tubing resonant response effect on the fluctuating pressures. The method outlined by Irwin *et al.* [13] was applied to the data. This method takes the known resonant response of the tubing system including the pressure transducer and filters the pressure data in the frequency domain to remove the resonant effects. The benefits of this method are that the data is corrected for both amplitude and phase distortion.

The sectional lift and drag forces were determined by integrating the pressure around the ring of pressure taps using equations (1) and (2). The sectional fluctuating forces were determined using the same formulae with the standard deviation fluctuating  $C_{p\sigma}$  substituted for the mean  $C_p$ ,

$$C_L = \frac{1}{2} \int_0^{2\pi} C_p \sin\theta \, d\theta \quad (1)$$

$$C_D = \frac{1}{2} \int_0^{2\pi} C_p \cos\theta \, d\theta \quad (2)$$

The correlation coefficients for the fluctuating pressures were determined using equation (3), therefore calculating the average correlation coefficient for the whole sample set,

$$\rho_{xy} = \frac{\overline{p_x p_y}}{\sigma_x \sigma_y} \quad (3)$$

The correlation coefficients were determined with respect to the center of the cylinders axis.

**RESULTS**

**Smooth Cylinders**

Experiments were conducted on smooth cylinders to provide a basis against which to compare the effect of surface roughness. Figure 1 presents the sectional mean drag coefficient for the smooth cylinders over a range of Reynolds numbers. The open and closed symbols in the figure represent data collected in the 1.5 MW and 450 kW wind tunnels

respectively. As expected for the range of Reynolds numbers the sectional mean drag decreases during the critical transition, although at a slightly lower Reynolds number than low turbulence flow due to the effect of the increased turbulence intensity of 3 % in the wind tunnels. After transition the mean drag begins to increase and towards the end of the experimental Reynolds number range shows a trend of beginning to plateau.

The sectional RMS fluctuating lift coefficients for the smooth cylinders in Figure 2 display a similar trend to the mean drag coefficient. The sectional fluctuating lift reaches a low value of 0.1 at critical transition before increasing as the Reynolds numbers progress through the supercritical regime. Between  $Re = 8 \times 10^5$  and  $1.2 \times 10^6$  the curve seems to plateau before decreasing for higher Reynolds numbers. Unfortunately, in Figures 1 and 2 the curves for the 100 mm and 400 mm cylinders fail to overlap by approximately a Reynolds number of  $0.5 \times 10^5$ .

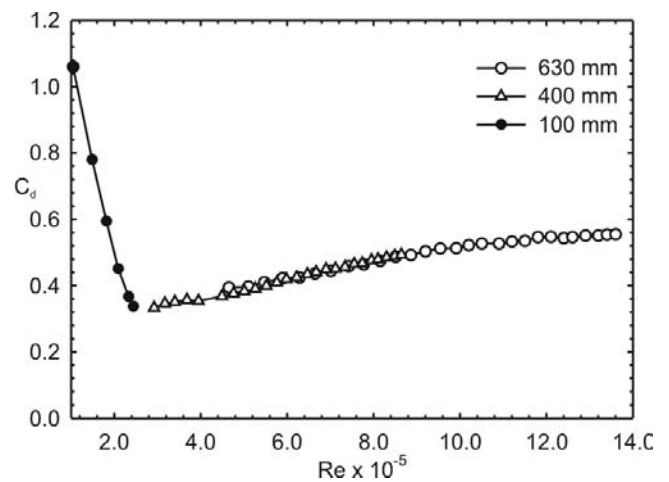


**Figure 1: Sectional mean drag coefficients for nominally smooth cylinders**

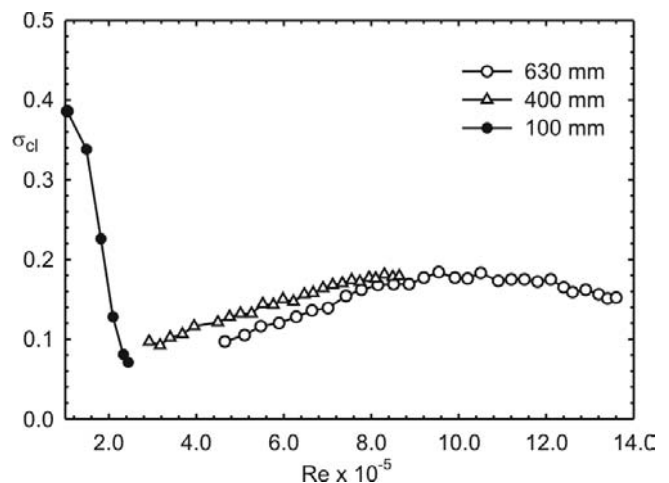


**Figure 2: Sectional RMS fluctuating lift coefficients for nominally smooth cylinders**

Figures 3 and 4 show the correlation of the pressures along the 90-degree generator for the 100 mm and 630 mm cylinders respectively for several of Reynolds numbers. The axial separation is based around the center of the cylinder span and increases to the left (negative separation) and right (positive separation) from this position. The correlation of the pressure decays quickly for the 100 mm cylinder over all Reynolds numbers. The correlation decreases with increasing Reynolds numbers, with negative correlation coefficients obtained for tap spacing between one and three diameters.

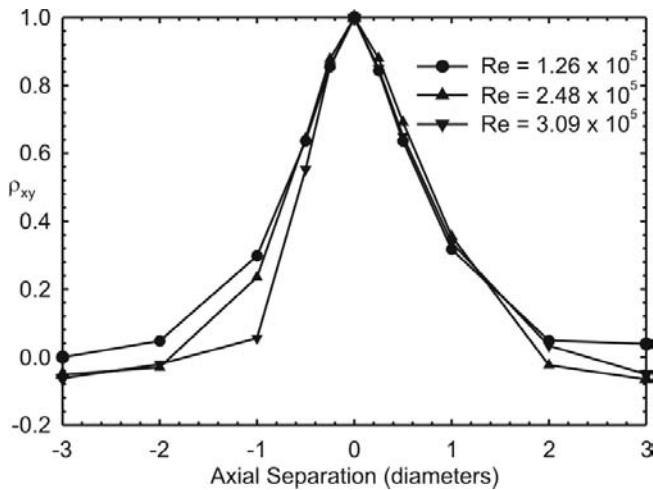


**Figure 3: Axial correlation coefficient for pressures along the 90-degree generator for the nominally smooth 100 mm cylinder**

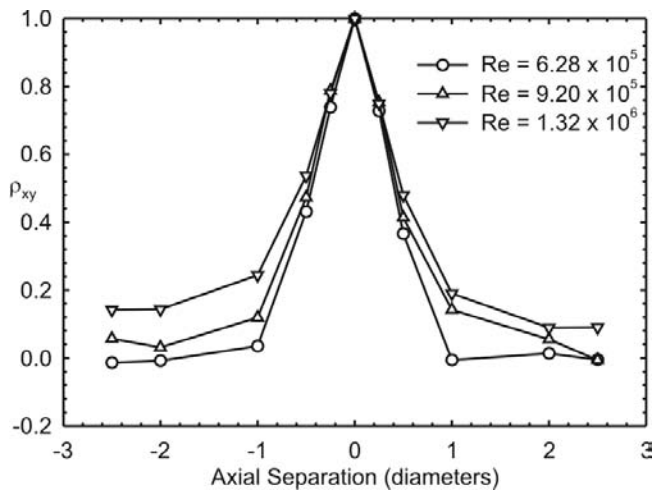


**Figure 4: Axial correlation coefficient for pressures along the 90-degree generator for the nominally smooth 630 mm cylinder**

The correlation coefficient curves for the 630 mm cylinder display a similar trend to that of the 100 mm cylinder curves, a rapid decay of correlation with axial separation. The correlation

of the pressures increases with Reynolds number as the flow regime progresses through the supercritical regime.

### **Rough Cylinders**

This section presents the results for cylinders of various surface roughness levels. In Figure 5 the sectional mean drag for the 100 mm cylinder increases with Reynolds number. The sectional mean drag coefficient has changed dramatically from the smooth cylinder presented in Figure 1. There is a noticeable gap in the data that is also apparent in the sectional fluctuating lift curve in Figure 6, which will be covered by the 400 mm rough cylinder data.

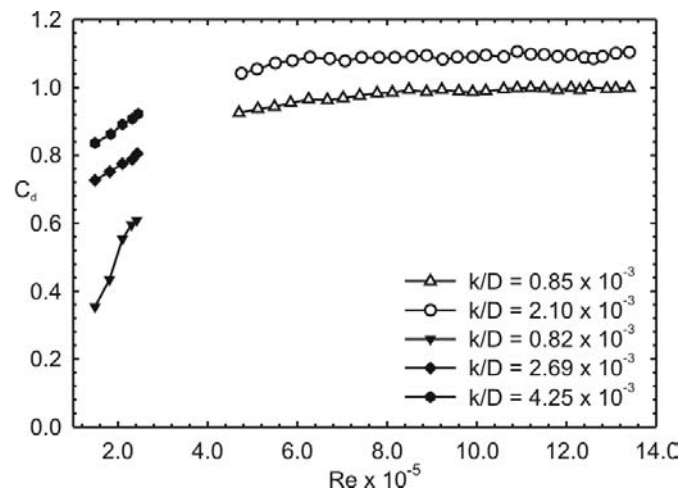


**Figure 5: Mean drag coefficients for rough cylinders**

At higher Reynolds numbers obtained with the 630 mm cylinder the drag coefficient initially increases then plateaus at approximately  $Re = 6 \times 10^5$ . The drag coefficient displays a dependence on the level of surface roughness, increasing with each rise in relative roughness. In fact, for the highest relative roughness on the 630 mm cylinder the drag coefficient is similar to that found on the smooth 100 mm cylinder at the lowest Reynolds number in Figure 1.

The sectional RMS fluctuating lift has similar trends to that of the mean drag, increasing with Reynolds number for the 100 mm cylinders and reaching a plateau at higher Reynolds number on the 630 mm cylinder (Figure 6). The peak value of the sectional RMS lift is twice that measured on the smooth cylinder under the same conditions. The lift does display a dependence on the level of surface roughness, but not to the same degree as the drag coefficient shown in Figure 5.

There seems to be a discrepancy in the data for the 100 mm cylinder with  $k/D = 0.82 \times 10^{-3}$ . The data do not display the same increasing trend to that of the rougher cylinders. It is thought this may be due to the type of sandpaper used and the method of determining the relative roughness of the cylinder, which will be discussed later.

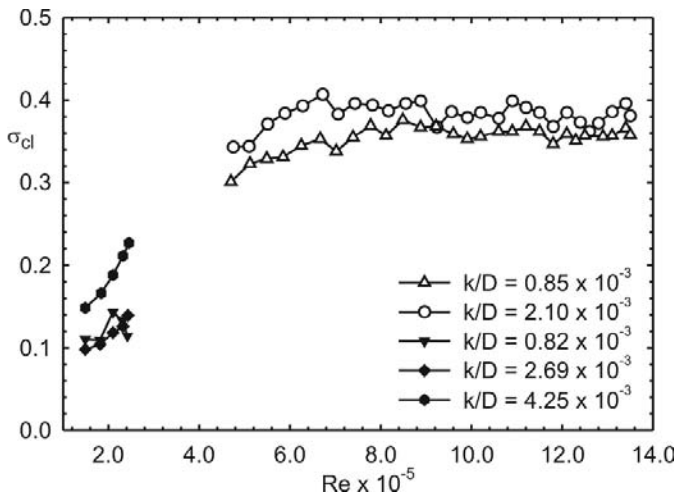


**Figure 6: RMS fluctuating lift coefficient for rough cylinders**

Figures 7 to 9, 10 and 11 present the correlation coefficients in order of increasing  $k/D$  for the 100 mm and 630 mm cylinders respectively. Comparing these figures with Figures 3 and 4 clearly indicates an increase in correlation of the pressures on the rough cylinders compared to the smooth cylinders. For the 100 mm cylinders the correlation increases with relative roughness. At the higher Reynolds numbers obtained using the 630 mm cylinder the correlation has increased further, although there is little difference between the curves in Figures 10 and 11.

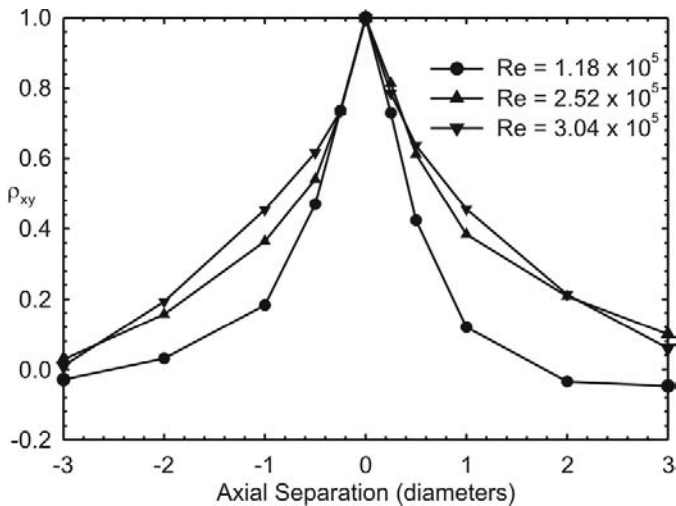


**Figure 7: Axial correlation coefficient for pressures along the 90-degree generator for  $k/D = 0.82 \times 10^{-3}$  100 mm cylinder**

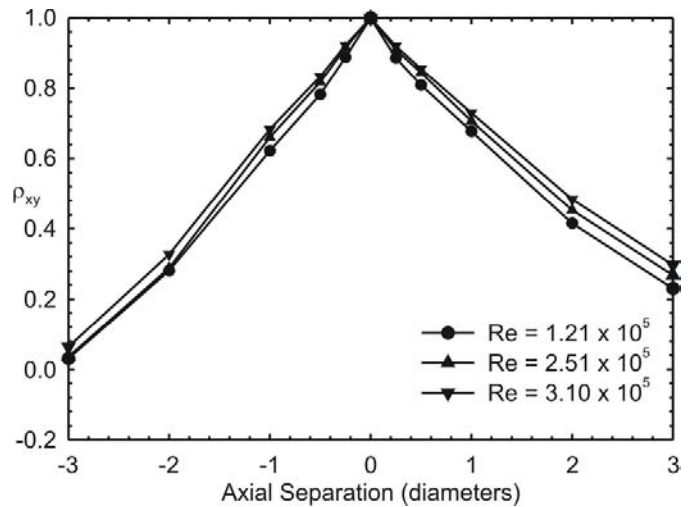


**Figure 8: Axial correlation coefficient for pressures along the 90-degree generator for  $k/D = 2.48 \times 10^{-3}$  100 mm cylinder**

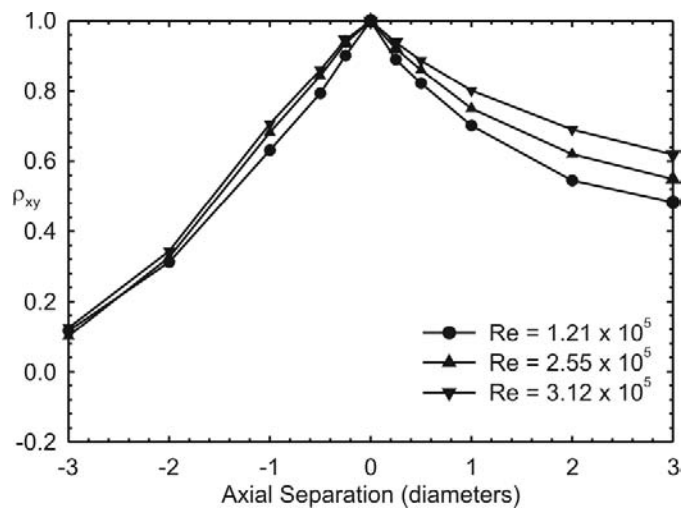


**Figure 9: Axial correlation coefficient for pressures along the 90-degree generator for  $k/D = 4.25 \times 10^{-3}$  100 mm cylinder**

## DISCUSSION

Previous research has shown the influence of surface roughness on the crosswind forces of a circular cylinder at critical and higher Reynolds numbers [4, 8, 9]. However, a majority of this work has measured the total crosswind forces on a finite length cylinder. Total forces are an integrated effect of the sectional force coefficient and the axial correlation of the sectional forces. Therefore, any change in total force could be the result of changes in either the sectional forces or the axial correlation of the forces. The aim of this investigation was to separate the effect of surface roughness on the sectional crosswind forces and correlation of these forces.

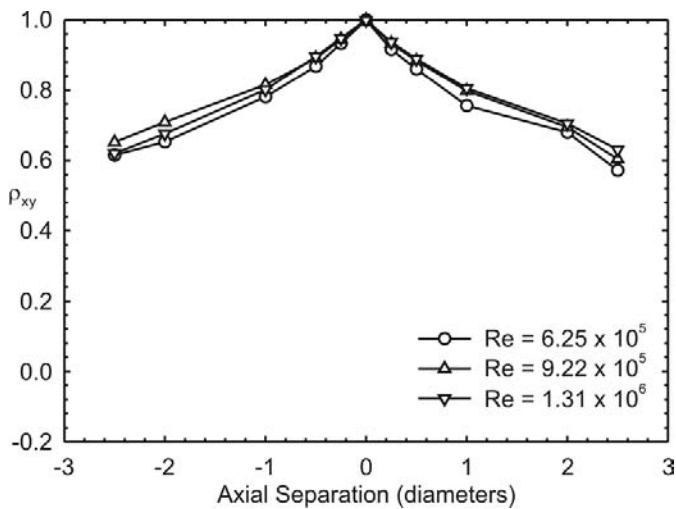


**Figure 10: Axial correlation coefficient for pressures along the 90-degree generator for  $k/D = 0.85 \times 10^{-3}$  630 mm cylinder**

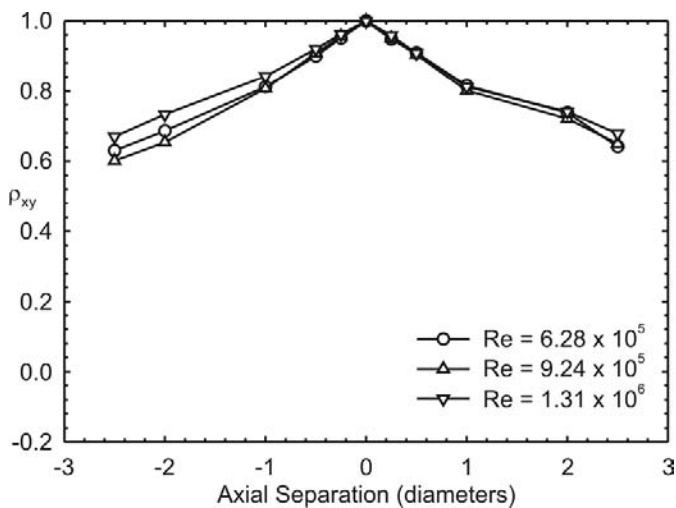


**Figure 11: Axial correlation coefficient for pressures along the 90-degree generator for  $k/D = 2.10 \times 10^{-3}$  630 mm cylinder**

The results for the smooth cylinder have shown the expected decrease in the sectional mean drag coefficient, RMS fluctuating lift coefficient and correlation of the pressures with Reynolds number, as the boundary layers on the cylinder transition to turbulence. After transition these parameters recover with the sectional mean drag beginning to plateau, the sectional RMS fluctuating lift beginning to decrease, and the correlation remaining relatively low at the highest Reynolds numbers.

The introduction of surface roughness has promoted turbulent transition in the boundary layers at a lower Reynolds numbers. The effect is pronounced on the sectional mean drag

coefficient where the curves for the 100 mm cylinders increase with Reynolds number and shift vertically for each increase in roughness. At Reynolds numbers above  $4 \times 10^5$  the drag coefficient has become independent of Reynolds number, being only a function of relative roughness. Achenbach and Heinecke [14] reported similar trends for the total drag on rough cylinders. They measured total drag coefficients as high as 1.25 on very rough cylinders. Guven *et al.* [15] suggested that the increased level of surface roughness promotes earlier separation, resulting in a wider wake and a higher mean drag coefficient.

The sectional RMS fluctuating lift coefficient was found to increase with surface roughness reaching values twice that measured on the smooth cylinder for the same Reynolds number. At the lower Reynolds numbers of the 100 mm cylinders, the fluctuating lift increases with Reynolds number and the curves shift vertically with increasing  $k/D$ . However, for a roughness of  $k/D = 0.82 \times 10^{-3}$  this trend was not observed. It is thought that the sandpaper used on the cylinder is responsible. Examining the paper revealed that the bonding agent used to attach the grit to the paper fills in the gaps between the grains to approximately 50% of their height. Therefore, the actual roughness of the cylinder is lower than the value determined using the average particle diameter. Unfortunately, there is still a lack of a single parameter to describe the level of surface roughness. Possibly using the hydrodynamic roughness may provide a better measurement of the relative roughness, but this still requires investigation.

At Reynolds numbers above  $4 \times 10^5$ , the sectional RMS fluctuating lift coefficient has leveled off at an elevated value compared to the smooth cylinder. It is now a weak function of Reynolds number and is dependent on the level of relative roughness. The increased turbulence intensity levels used in these experiments could affect the sectional RMS fluctuating lift coefficient. Cheung (1983) showed that the influence of free stream turbulence on the total fluctuating lift coefficient increased with the level of relative roughness. The elevated value of the sectional fluctuating lift found in these experiments is due to this rather than the influence of surface roughness. Sectional lift data has been collected for the 100 mm cylinders at  $I = 0.6\%$  and will be reported in future papers.

The measurements of the axial correlation of the pressures at Reynolds numbers above  $4 \times 10^5$  is some of the first data available for rough cylinders. It has been clearly shown that the axial correlation has a strong dependence on the level of surface roughness. At the lower Reynolds numbers and low relative roughness, the correlation increases with Reynolds number as the boundary layer completes transition but, at higher roughness, there is very little dependence on Reynolds number. At Reynolds numbers above  $4 \times 10^5$  the pressures are extremely well correlated along the generator. Batham [11] suggested that the separation and vortex shedding from the cylinder is two-dimensional, rather than three-dimensional as is found on a smooth cylinder at similar Reynolds numbers. The results of the correlation measurements confirm this.

The combined effect of elevated sectional fluctuating lift coefficient and higher correlation of the pressures along the cylinder will result in a significantly higher total lift force on rough cylinders compared to smooth cylinders. This could explain the violent vibrations that were observed during the rough cylinder experiments here, and those reported by Shih *et al.* [10] and Zhang [9].

Further experiments are required to close the small gap in Reynolds numbers between the 100 mm and 400 mm cylinders data and determine the combined effect of roughness and free stream turbulence on the crosswind forces.

## CONCLUSIONS

The result here agreed with previous studies, which show that smooth cylinder results display the trends commonly found for cylinders in the critical and supercritical regimes. The sectional mean drag coefficient, sectional RMS lift coefficient and correlation of pressures decrease during critical transition and then recover to slightly higher values in the supercritical regime.

The presence of surface roughness has a significant effect on the flow around the cylinder. The correlation of pressures increased with relative roughness, approaching values found in the high subcritical regime. The higher correlation of the pressures confirms Batham's [11] suggestion that the separation and vortex shedding from a rough cylinder was more two dimensional than the more three dimensional nature of a smooth cylinder at similar Reynolds number.

It is believed that the sectional fluctuating lift coefficient on the rough cylinders was increased due to the improved interaction between the free stream turbulence and the cylinder flow field.

The combination of an increased axial correlation of the pressures and elevated sectional RMS fluctuating lift will result on increased vortex-induced vibration on rough cylinders. This provides an explanation for the vibrations observed during these experiments and those by Zhang [9] and Shih *et al* [10].

## REFERENCES

1. Roshko, A., 1961, "Experiments on the flow past a circular cylinder at very high Reynolds number": *Journal of Fluid Mechanics*, **10**, pp. 345-356.
2. Fage, A. and Warsap, J. H., 1929, "The effects of turbulence and surface roughness on the drag of a circular cylinder," Report and Memoranda 1283, Aeronautical Research Council, 7.
3. Schewe, G., 1986, "Sensitivity of transition phenomena to small perturbations in flow round a circular cylinder": *Journal of Fluid Mechanics*, **172**, pp. 33-46.
4. Szechenyi, E., 1975, "Supercritical Reynolds number simulation for two-dimensional flow over circular cylinders": *Journal of Fluid Mechanics*, **70**, pp. 1975.
5. Nakamura, Y. and Tomonari, Y., 1982, "The effects of surface roughness on the flow past circular cylinders at high Reynolds numbers": *Journal of Fluid Mechanics*, **123**, pp. 363-378.
6. Buresti, G., 1981, "The effect of surface roughness on the flow regime around circular cylinders": *Journal of Wind Engineering and Industrial Aerodynamics*, **8**, pp. 105-114.
7. Ribeiro, J. L. D., 1991, "Effects of surface roughness on the two-dimensional flow past circular cylinders II: fluctuating forces and pressures": *Journal of Wind Engineering and Industrial Aerodynamics*, **37**, pp. 311-326.
8. Cheung, C. K., 1983, "Effect of turbulence on the aerodynamics and response of a circular structure in wind flow," PhD Thesis, Monash University, Clayton.
9. Zhang, H., 1993, "Flow interference between two circular cylinders in turbulent flow," PhD, Monash University, Melbourne.
10. Shih, W. C. L., Wang, M. C., Coles, D. and Roshko, A., 1993, "Experiments on flow past rough circular cylinders at large Reynolds Numbers": *Journal of Wind Engineering and Industrial Aerodynamics*, **49**, pp. 351-368.
11. Batham, J. P., 1973, "Pressure distributions on circular cylinders at critical Reynolds numbers": *Journal of Fluid Mechanics*, **57**, pp. 209-228.
12. Engineering Sciences Data Unit, 1996, "Response of Structures to Vortex Shedding: Structures of Circular or Polygonal Cross Section," 96030, ESDU International, 65.
13. Irwin, H. P. A. H., Cooper, K. R. and Girard, R., 1979, "Correction of distortion effects caused by tubing systems in measurements of fluctuating pressures": *Journal of Wind Engineering and Industrial Aerodynamics*, **5**, pp. 93-107.
14. Achenbach, E. and Heinecke, E., 1981, "On vortex shedding from smooth and rough cylinders in the range of Reynolds number  $6 \times 10^3$  to  $5 \times 10^6$ ": *Journal of Fluid Mechanics*, **109**, pp. 239-251.
15. Guven, O., Farrell, C. and Patel, V. C., 1980, "Surface roughness effects on the mean flow past circular cylinders": *Journal of Fluid Mechanics*, **98**, pp. 673-701.